Evolution of Sigma Phase in 321 Grade Austenitic Stainless Steel Parent and Weld Metal with a Duplex Microstructure

Authors: Graham Green[1], Dr Rebecca Higginson[1], Dr Simon Hogg[1], Dr Sarah Spindler[2] and Dr Chris Hamm[2]

[1] Department of Materials, Loughborough University, Loughborough, LE11 3TU, UK

[2] EDF Energy, Barnett Way, Barnwood, Gloucester, GL4 3RS, UK

Contact: G.Green@lboro.ac.uk

Keywords: Sigma phase, 321, Stainless steel, Microstuctural Development, Precipitation, Particle Size

Abstract

Samples of 321 stainless steel from both the parent and welded section of a thin section tube were subjected to accelerated ageing to simulate long term service conditions in an Advanced Gas Cooled Reactor (AGR) power plant. The initial condition of the parent metal showed a duplex microstructure with approximately 50% ferrite and 50% austenite. The weld metal showed three distinct matrix phases, austenite, delta ferrite and ferrite. This result was surprising as the initial condition of the parent metal was expected to be fully austenitic and austenite + delta ferrite in the weldment. The intermetallic sigma phase formed during the accelerated ageing was imaged using ion beam induced secondary electrons then measured using computer software which gave the particle size as a function of ageing time. The measurements were used to plot particle size, area coverage against ageing time and minimum particle spacing for the parent metal. During ageing the amount of ferrite in the parent metal actually increased from ~50% to ~80% after ageing for 15,000 hours at 750°C. Sigma has been observed to form on the austenite/ferrite boundaries as they may provide new nucleation sites for sigma phase precipitation. This has resulted in small sigma phase

particles forming on the austenite/ferrite boundaries in the parent metal as the ferrite transforms from the austenite.

Introduction

Stainless steels frequently see use in the power industry due to the requirement of maintaining mechanical properties, corrosion and oxidation resistance at elevated temperatures.[1,] To achieve these properties, the Advanced Gas Cooled Reactor (AGR) power stations, built ~30 years ago, use various grades of stainless steel in the build. However many of these power stations are due to be decommissioned in the next 10-20 years and to extend the service life beyond the initially planned decommission date the effect of prolonged exposure to in-service conditions must be understood. Components made with stainless steel, such as steam conveyance tubing, are subjected to high temperature and pressure steam. The high temperatures involved in the operation of the power plant causes the stainless steel to transform at an accelerated rate towards its equilibrium state. The equilibrium state of a material can be modelled by using software such as Thermocalc with a suitable database, which takes an input of chemistry and predicts the stable phases over a temperature range. The predominant intemetallic phase to form during ageing in a 321 grade austenitic stainless steel is sigma (σ) phase.[2,] Pre-service, the material is given a heat treatment with the aim of producing fully austenitic steel. The addition of titanium is primarily to stabilise the steel as it is known to have the effect of reducing the precipitation of chromium rich carbides, this reduces the sensitisation effect as well as decreasing the time taken to form σ.[3,] These titanium carbo-nitrides remain after solution heat treatments and affect the subsequent precipitation sequence. The formation of σ and other intermetallic phases cause the component to have a reduction in fracture toughness due to the brittle nature and location of the particles, primarily on grain boundaries, which allows cracks to readily propagate through the metal.[4,] Sigma phase has been seen to form in 321 stainless steel after accelerated ageing with the chemistry 58.4wt% Fe, 36wt% Cr and 5.6wt% Ni. σ can form in both austenitic and ferritic steels over a

temperature range 650°C-750°C[5] and is documented to reduce the toughness and the ductility of the material, these properties worsening as the size of the intermetallic increases. It is important to understand the formation of the σ-phase in the 321 stainless steel as the reduction in fracture toughness may lead to failure of critical components.

The formation of precipitates in the metal is further complicated in welded regions. Austenitic welds are designed to contain a portion (~10%) of delta ferrite to avoid hot cracking.[6,] Delta ferrite is known to transform to σ more quickly than austenite due to having a BCC crystal structure[7,] which allows faster diffusion than the FCC austenite due to being less close-packed, as well as being richer in chromium than the austenitic matrix. σ has been observed to form during multipass welding[7,] and so post weld heat treatments are often used to dissolve intemetallics and delta ferrite.

Due to the stainless steel components being designed to operate for over 30 years at temperatures up to ~650°C it is not practical to perform laboratory experiments at this temperature as the times involved are beyond the scope of most work, instead a higher temperature is used to simulate prolonged exposure in a shorter time. Using a higher temperature to age materials can produce problems, for example a variance in phase stability which can result in the formation of phases that would not otherwise form while at service temperatures. This could potentially result in difficulties when comparing the samples. This paper aims to investigate the formation of σ in an austenitic stainless steel when aged at 750°C in laboratory conditions.

Experimental

The 321 material was supplied as thin section tube with an autogenous helical weld. The measured chemistry of the parent and the weld metal are shown in Table 1. This was used as the input for the thermodynamic modelling with Thermocalc using the TCFE 6 database.

The material was sectioned and encapsulated in quartz tubing back filled with argon to prevent oxidation of the material during ageing. Accelerated ageing of the material was performed at 750°C and removed at various times up to 15,000 hours.

After ageing the materials were mounted in bakelite, ground and polished to a 1µm finish then given a final polish with colloidal silica. The intemetallic particles were imaged using ion beam induced secondary electrons in a Focused Ion Beam Secondary Electron Microscope (FIBSEM). This method of imaging was used as it provides good contrast between the matrix and the particles. Quantification of the particle size and area fraction was achieved by running the images through Uthesca image tool. The particle size was calculated as equivalent round diameters in micrometres. The minimum inter-particle spacing was calculated using a MatLab script.

Table 1: Measured chemistry of the bulk parent and weld metal, chemistry measured by inductively coupled plasma optical emission spectroscopy (ICP-OES). Amount measured in wt-%.

Location	C	Si	Mn	P	S	Cr	Mo	Ni	Ti	Cu
Parent	0.046	0.56	1.53	0.019	0.01	17.38	0.45	8.92	0.33	<0.01
Weld	0.04	0.31	0.86	0.011	0.016	18.54	2.56	11.38	<0.005	0.4

Results and discussion

The intemetallic phase that is predicted to form with the largest mass fraction in this stainless steel is σ, this is shown in the phase plot in Figure 1 which agrees with the literature on other titanium stabilised stainless steels. There is a small amount of $M_{23}C_6$ predicted to form, this is due to the presence of titanium preferentially forming the titanium carbo-nitrides but the remaining carbon in solid solution can form a small amount of chromium rich carbides. The thermocalc result has shown that σ forms more prolifically than the other second phases and is also known to be the most deleterious to the mechanical properties, and as such is the only second that is required to be identified when analysis the aged metals in this work. At 750°C which is the accelerated ageing temperature used for this material, Thermocalc predicts 9.6% σ at equilibrium. Ion beam imaging can be used to provide excellent contrast between the matrix and a non-conductive second phase (σ).

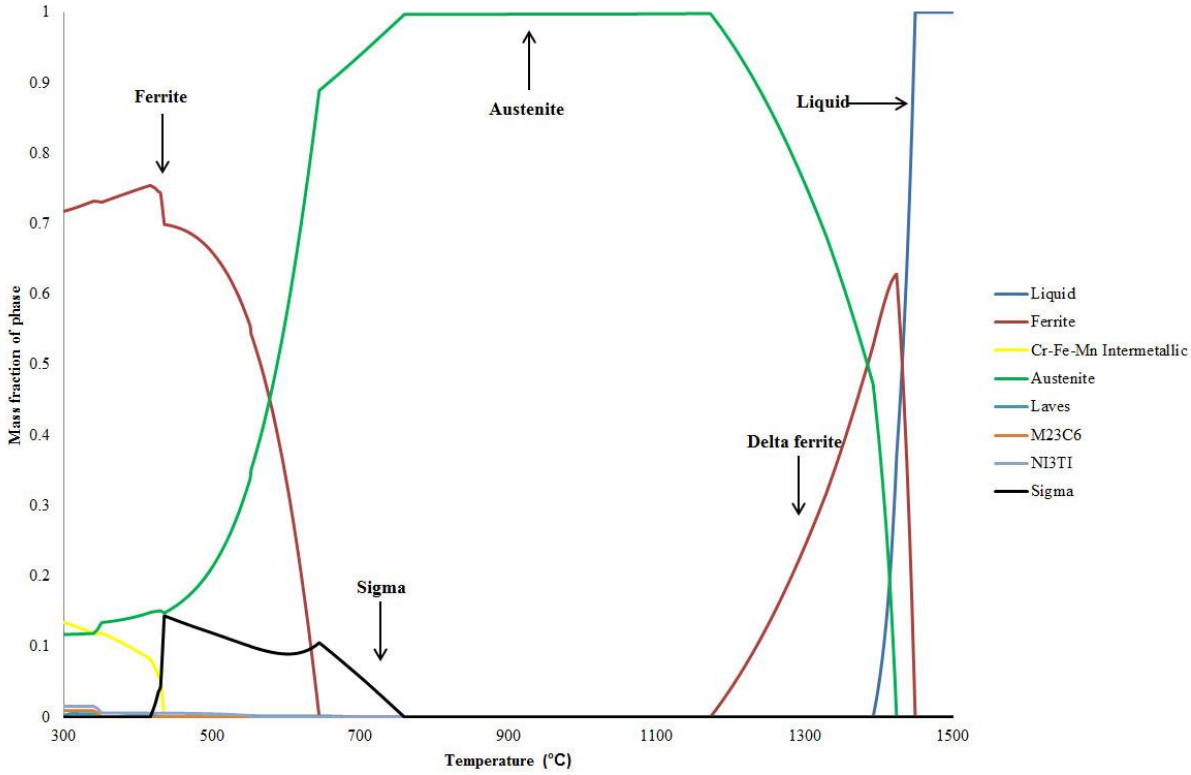

Figure 1: Predicted stable phases in 321 steel. The diagram was constructed using Thermocalc with the TCFE database, the measured chemistry shown in Table 1 was used as the input.

The as-received material was characterised to understand the subsequent ageing treatments. The parent metal shown in Figure 2 (a) shows a duplex structure in the EBSD phase map, composed of ~50% ferrite and 50% austenite grains. The austenite grains were measured to be ~10 μm in size but the ferrite regions were found to have a varied morphology so accurate grain size measurements are difficult. Titanium carbide particles can be seen and are labelled in Figure 2 (a). The titanium carbides are shown in green as they share the same FCC crystal structure as the austenite; these carbides are formed during the solution heat treatment of the steel to reduce the amount of carbon in solid solution in the matrix. The material was thought to be a fully austenitic, as all the 300 series stainless steels are all specified to be fully austenitic. In the case of this parent metal there is a large fraction of ferrite in the matrix which, amongst other effects could change the ageing characteristics of the material. A low magnification EBSD phase map of the weld metal is shown in Figure 2 (b) where it can be seen that there is a vermicular formation of ferrite and large austenite grains. The as-received weld metal contains three matrix phases as shown in Figure 3. Based on the EDS results in Figure 3, the delta ferrite is high in chromium but there is another ferrite phase that has a similar chromium and nickel content to the austenite. This suggests that the other phase in the weld metal has formed displacively from the austenite. 321 grade stainless steel has been reported to form martensite on deformation[8,] however this material has not been deformed after having a standard austenising heat treatment and does not have a typical lath/plate martensite morphology so has been labelled as ferrite. This result will be discussed in more detail in another paper.

As predicted by Thermocalc, σ forms on thermal ageing, and has been identified after only 100 hours of ageing at 750°C. σ particles were identified by extraction from an etched sample using carbon replicas. These replicas were then analysed in a TEM and the chemistry and diffraction patterns analysed. An image of a σ particle along with the chemistry determined by EDS and a diffraction pattern are shown in Figure 4.

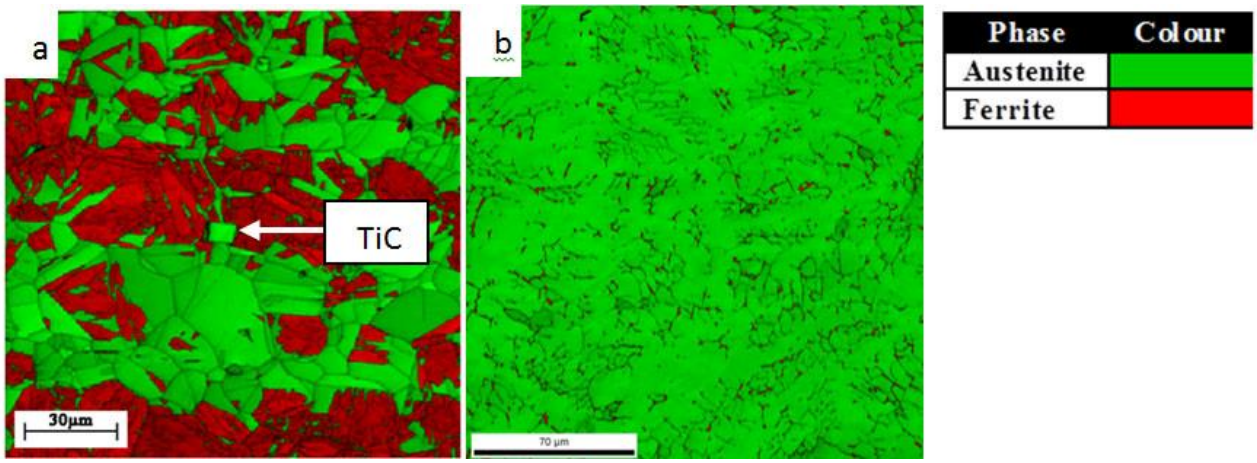

Figure 2: EBSD phase map for the 321 parent metal (a) and 321 weld metal (b). The parent metal shows a duplex structure, with green FCC grains and the red BCC phase, the weld metal has a more typical structure with large columnar austenite grains and a vermicular delta ferrite.

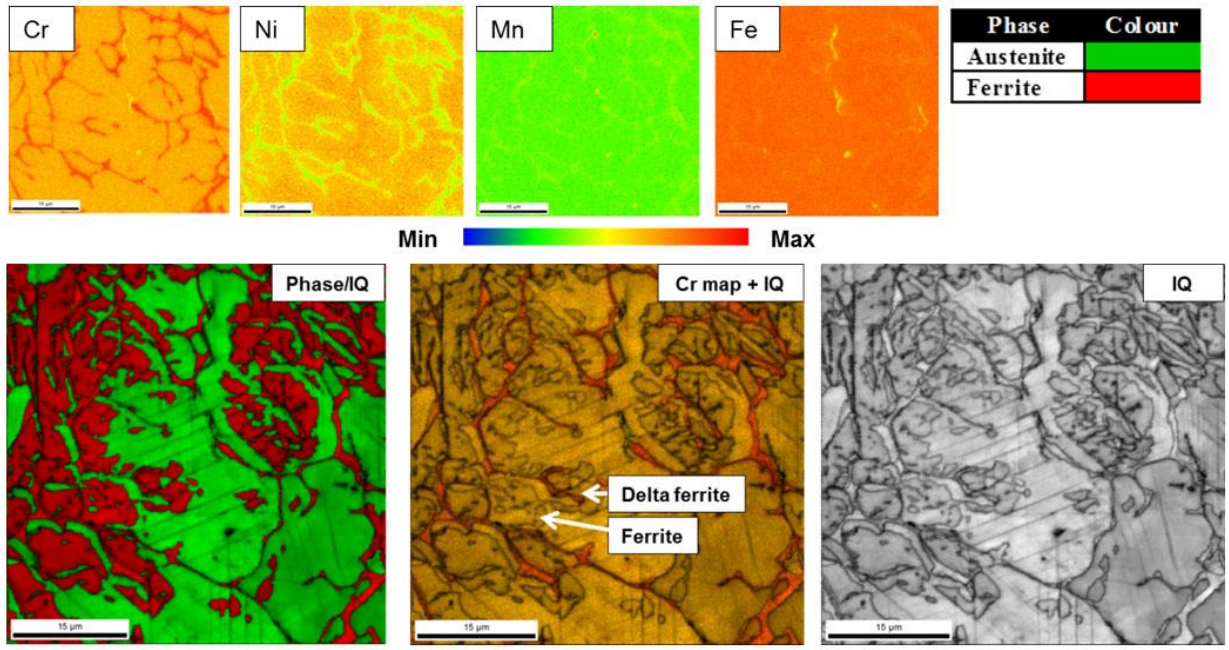

Figure 3: Combined EBSD and EDS map of the weld metal, showing delta ferrite with a high chromium content and ferrite with no discernible chemical difference to the austenite.

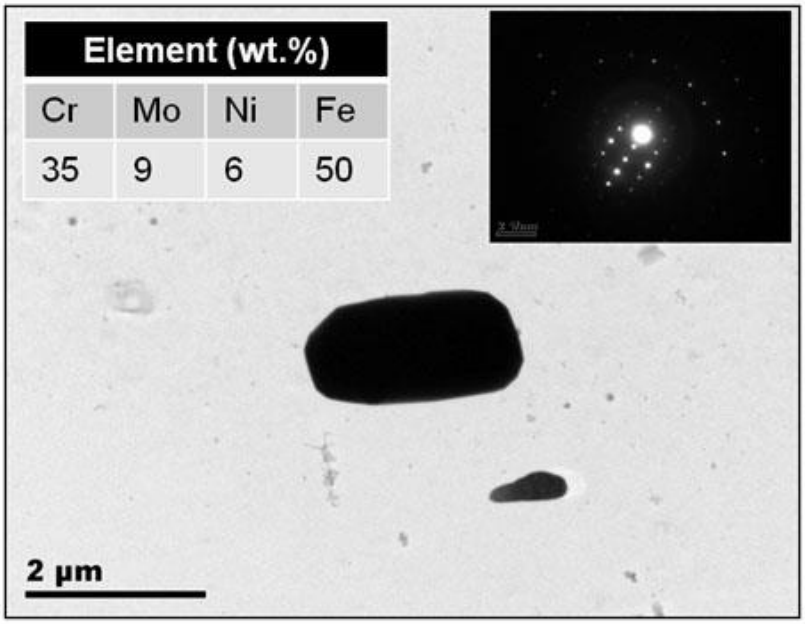

Figure 4: A σ particle imaged in a TEM with accompanying diffraction pattern and chemistry determined via EDS.

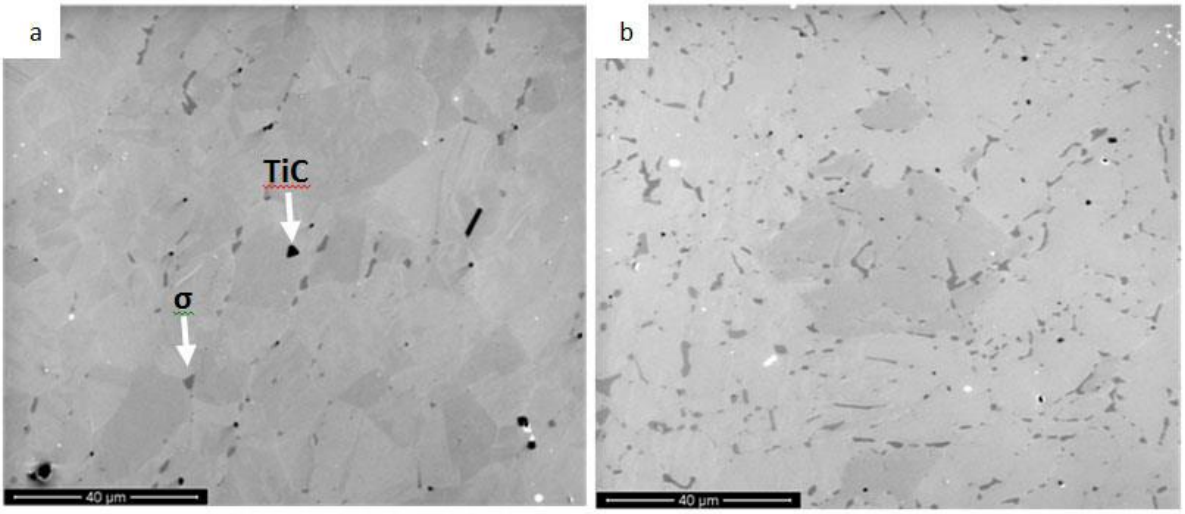

Figure 5: Ion beam images of the parent (a) and the weld metal (b) after ageing at 750°C for 100 hours. There are two particles, the darkest being titanium carbo-nitrides and the other is σ. Ion beam imaging was selected for the imaging technique for these materials as it can produce contrast between the matrix material and the second phases without requiring an etching technique which can introduce depth effects into micrographs.

The ion beam induced secondary electron images in Figure 5 show the intermetallic σ particles in dark contrast compared to the matrix and the titanium carbides as the blackest particles. Figure 5 shows that after 100 hours of ageing at 750°C both the parent (a) and the weld metal (b) show σ precipitation, however the weld metal shows substantially more precipitation than the parent. The software used to analyse the particles requires the images

to be thresholded. The ion beam images were thresholded removing the matrix material and leaving only the σ particles prior to image analysis, the TiC particles were manually removed from the image as the contrast and morphology were noticeably different from σ.

The images in Figure 6 show the evolution of particle size in the parent metal with ageing at 750°C. Sigma phase is shown to form at ageing times of less than 100 hours; this is due to the absence of $M_{23}C_6$ carbides on the grain boundaries. The absence of these carbides means that there is a larger amount of free chromium in the matrix which is available to form the σ. This is noticeable when comparing the stabilised 321 steel to the high carbon 316 steel which forms carbides after just 10 hours of ageing at 750°C and does not start to form σ until after 2,000 hours of ageing.[9,] The images show that the particle size rapidly increases until 2,000 hours at which point the increase in particle size is linear to 15,000 hours of ageing. There are small σ particles at all ageing times. The increasing ferrite fraction with ageing time may be providing new nucleation sites for sigma phase precipitation which could be due to the increased diffusion rate in the BCC ferrite as well as the creation of new boundaries. The thresholded images in Figure 7 show that σ forms more rapidly in the weld metal than in the parent metal. The reason for the rapid formation of σ is due to the presence of delta ferrite islands which are enriched with chromium. The higher chromium regions allow σ to rapidly form due to the chemical similarity between the two phases. Like the parent metal, σ in the weld metal shows fast growth until 2,000 hours at which point the growth rate slows down but then rapidly increase in size between 10,000 and 15,000 hours of ageing. The nucleation of the σ particles is primarily in the delta ferrite; this can be seen in Figure 7 where the morphology of the σ resembles the initial microstructure of the delta ferrite in the weld metal. As the ageing time increases, σ also forms on the austenite/austenite boundaries.

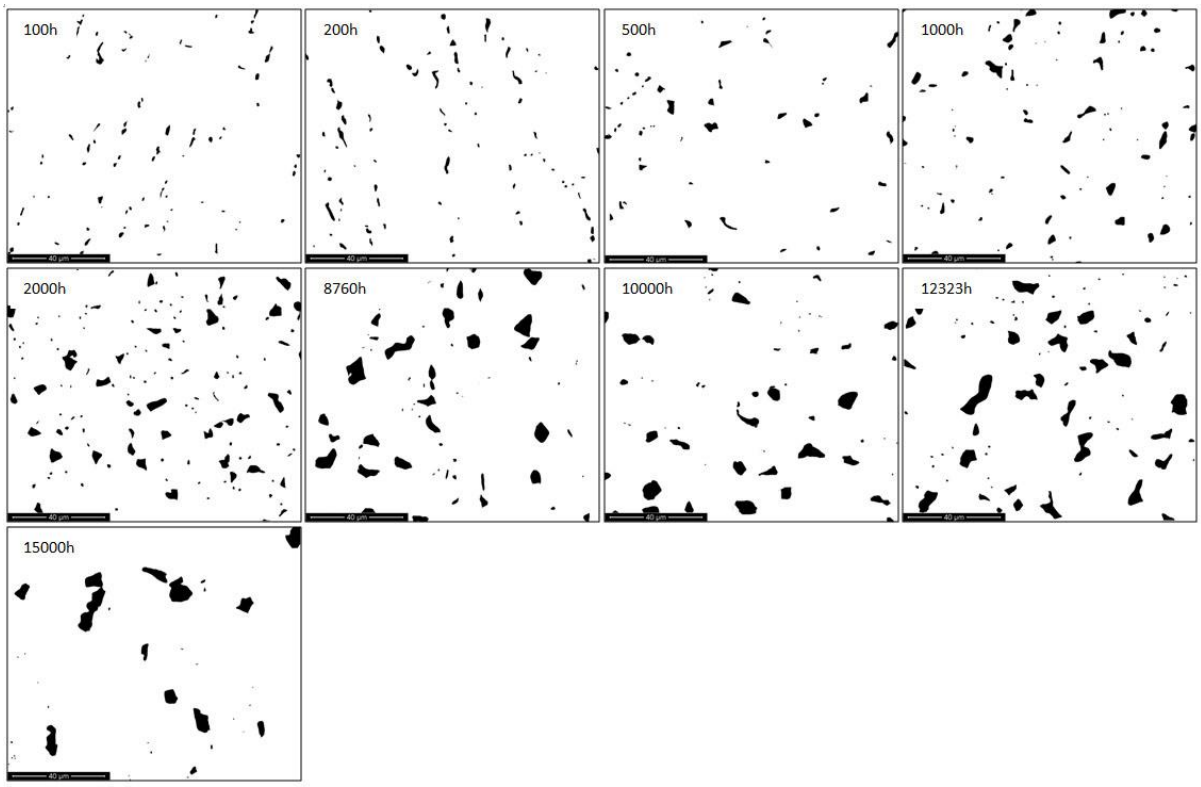

Figure 6: Typical result of thresholding the ion beam images of the σ in the parent metal. These images show an obvious trend of particle size increasing with ageing time.

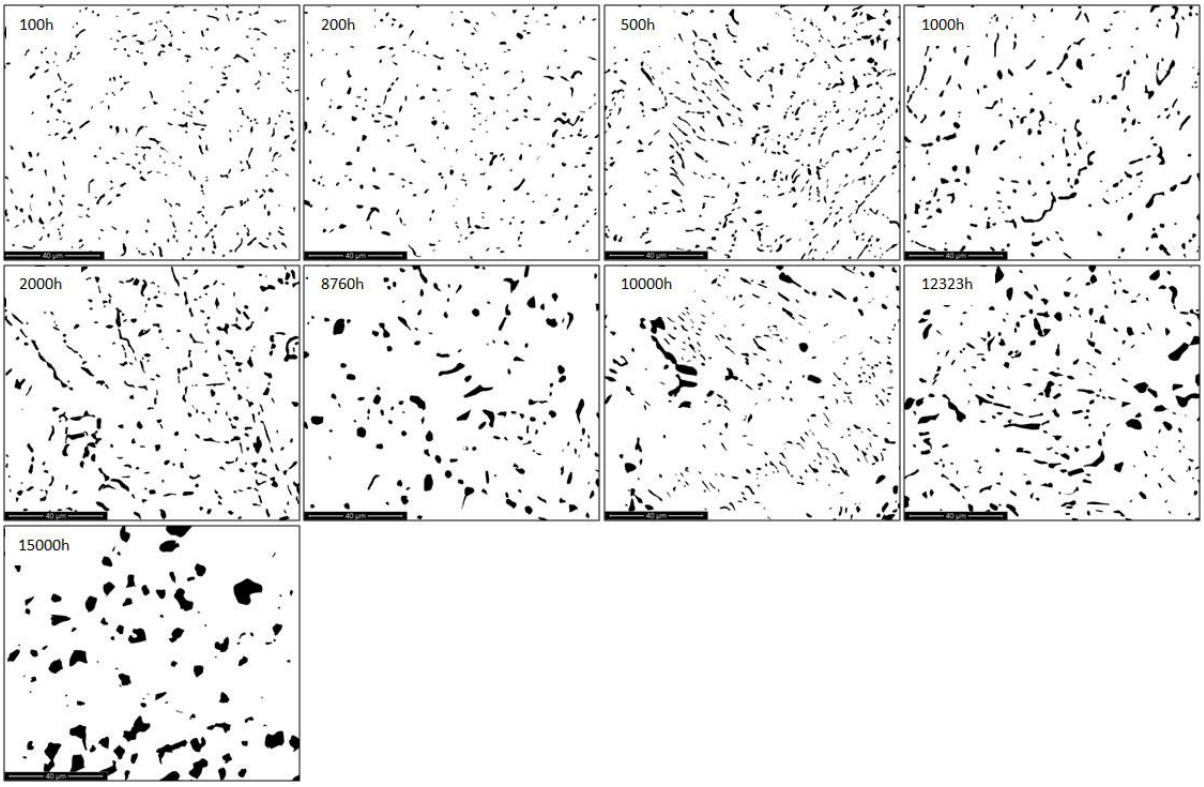

Figure 7: The result of thresholding the ion beam images of the σ in the weld. These images show an obvious trend of particle size increasing with ageing time.

Ion beam imaging is a powerful technique for analysing the σ particles but has limited use for determining how they relate to the matrix microstructure. The EBSD data in Figure 8 shows the relationship of the σ particles to the matrix in both the parent and the weld metals. In the parent metal the σ has formed on an austenite/ferrite boundary but has also formed on the austenite/austenite boundaries in other areas of the sample. The weld metal shows σ to have formed primarily in the prior delta ferrite regions, these are identified as they have a similar morphology to the delta ferrite in the unaged condition. It is also interesting to note that the area fraction of the ferrite in the weld metal has increased and can be identified primarily around the σ particles.

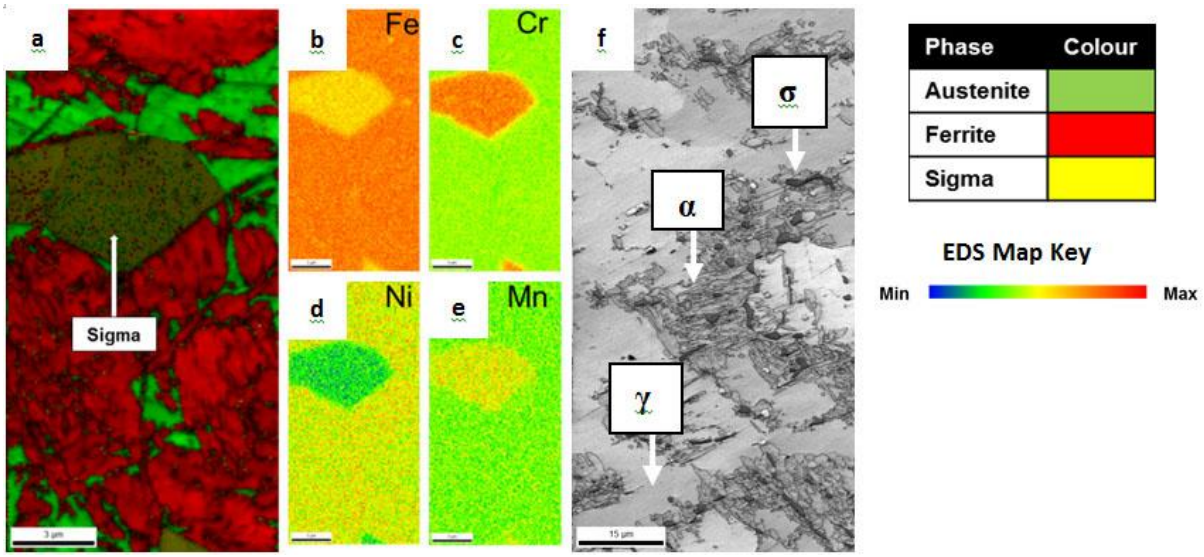

Figure 8: (a) EBSD phase map of a σ particle that has formed on the austenite/ferrite interface in the 321 parent metal after ageing for 12000 hours at 750°C with accompanying EDS maps (b-e). (f) EBSD image quality map of the weld metal after ageing for 12000 hours at 750°C, σ has formed on the austenite/ferrite boundaries and also in the prior delta ferrite regions.

At least 500 particles from each sample at each ageing time were imaged and measured in order to calculate the average particle diameter and the average area coverage of particles. A plot of the particle size against ageing time is shown in Figure 7 with results from the parent and weld metal. It shows that there is rapid particle growth until 2,000 hours of ageing after which the average particle size stays mostly constant in the weld metal. The particle

size increases relatively slowly in the parent between 2,000 and 12,000 hours then the average particle size rapidly increased again at 15,000 hours. This trend of particle size increase was shared with the weld metal. The area coverage of the parent and weld metals is also shown in Figure 7 where it can be seen that the amount of σ also increases with the particle size, although the amount of σ is greater in the weld rather than the parent metal despite the average particle size being greater in the parent than the weld metal. This may be due to the initial presence of delta ferrite in the weld metal allowing for rapid transformation to σ. This result is consistent with Minami *et al.* who observed rapid growth of σ at 1,000 hours at 700°C in a high carbon 321 grade stainless steel , however they found that after 10,000 hours at 700°C the total precipitation amount was less than 3% area coverage compared to over 5% as seen in this report.[10,] This difference is largely due to the ageing temperature as well as minor influences such as a larger grain size and higher carbon content and it is thought that the duplex ferrite/austenite microstructure increases the propensity to form σ in the materials studied in this report. As well as particle size, the spacing between the particles is important for predicting mechanical properties, especially creep properties.[11,] The fraction of σ measured by image analysis was 5.1% in the parent metal and 10.3% in the weld metal after 15,000 hours of ageing at 750°C; the Thermocalc results predict that there will be 9.6% σ at equilibrium. This shows that the parent metal is further from equilibrium than the weld metal, which is nearing the predicted equilibrium state. This data is going to be used to help validate a creep model which uses particle size and spacing. The particle spacing data for the parent metal is shown in Figure 10. The particle spacing is the minimum distance between the centre of a particle (minus the radius of the particle) and the nearest particle to it (minus the radius of the particle). It shows that the space between the particles increases rapidly for 1,000 hours, then reaches an approximately steady state until 10,000 hours then rapidly increases to 12,000 hours. The spacing data has not been calculated for the weld metal as the particle shape is far from spherical and the results can become skewed as the MatLab script assumes the particles are all spherical for simplicity.

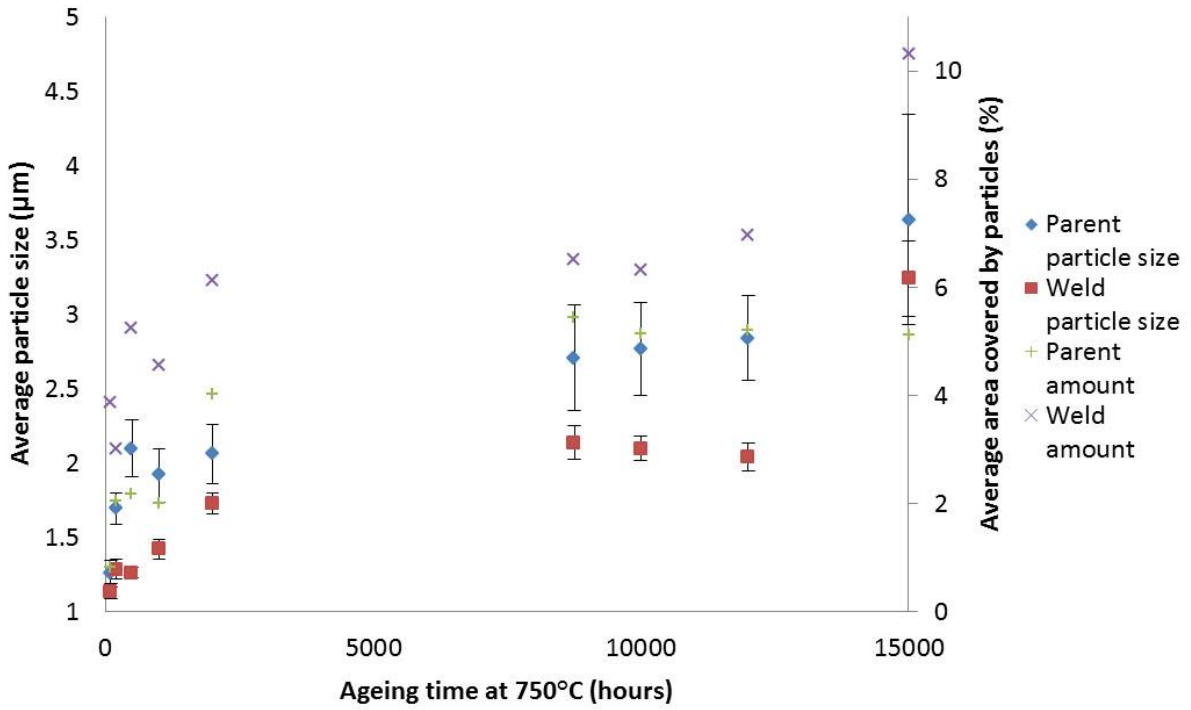

Figure 9: The thresholded ion beam images were analysed in Uthesca Image Tool. This software produces particle size data (feret diameter) and the area covered by particles. The plot shows data for the parent and weld metal when aged at 750°C for times of up to 15000 hours.

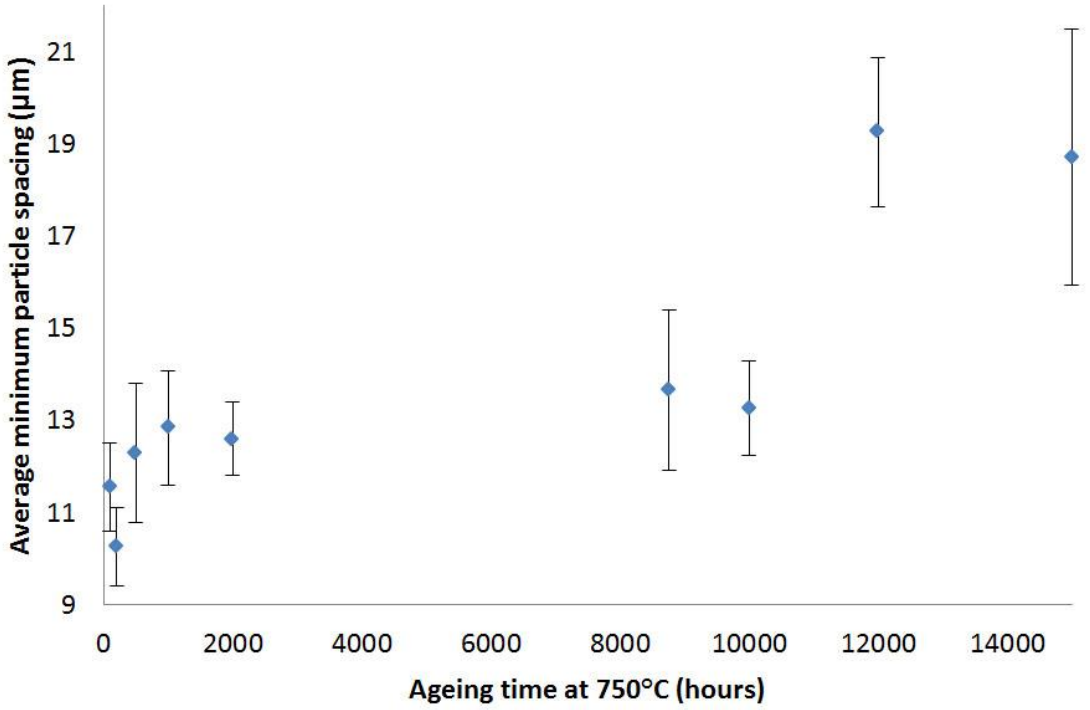

Figure 10: The average minimum particle spacing for the 321 grade parent metal determined by particle analysis of the ion beam images

Conclusions

The initial condition of the parent metal showed a duplex matrix microstructure with approximately 50% ferrite. The weld metal showed three matrix distinct phases, austenite, delta ferrite and ferrite. This was an unexpected result as the parent metal was thought to be fully austenitic and austenite + delta ferrite in the weldment.

Intermetallic σ formed rapidly during ageing, as was predicted by the thermodynamic data. The σ was imaged using ion beam induced secondary electrons, and then analysed using image analysis to determine the particle size and spacing. The measured fraction of σ was 5.1% in the parent metal and 10.3% in the weld metal after 15,000 hours of ageing at 750°C. The Thermocalc data showed that the fraction of σ at predicted equilibrium was 9.6%, the weld metal can be assumed to be at equilibrium while the parent metal has not yet reached this state.

The microstructure of the σ in the weld metal was similar to the delta ferrite morphology shown in the initial condition of the weldment. This was due to the enrichment of chromium in the delta ferrite which provided sites for σ to rapidly form.

During ageing the amount of ferrite in the parent metal increased. This is thought to provide new nucleation sites for σ precipitation. In the weld metal the amount of ferrite also increased and seemed to grow out from the prior delta ferrite regions.

Acknowledgements

The authors would like to thank EDF Energy and Loughborough University for providing the funding and the materials for this project.

References

1. W.J. Mills: ‘Heat-to-heat variations in the fracture toughness of austenitic stainless steels’ Eng. Fract. Mech., 1988, 30, 469–492

2. J. K. L. Lai: ‘Precipitate phases in type 321 steel’, J. Mater. Sci. Technol., 1985, 1, 97-100

3. K. Guan, X. Xu, H. Xu and Z. Wang: ‘Effect of aging at 700°C on precipitation and toughness of AISI 321 and AISI 347 austenitic stainless steel welds’, NUCL. ENG. DES., 2005, 235, 2485–2494

4. I.J. O'Donnell, H. Huthmann and A.A. Tavassoli: ‘The fracture toughness behaviour of austenitic steels and weld metal including the effects of thermal ageing and irradiation’, INT. J. PRES. VES. PIP., 1996, 65, 209-220

5. J. L. Hau and A. Seijas: ‘Sigma Phase Embrittlement of Stainless Steel in FCC Service’, Corrosion 2006, San Diego Ca, USA, March 2006, NACE International

6. K. P. Rao: ‘Effect of weld cooling rate on delta-ferrite content of austenitic weld metals’, J. Mater. Sci. Lett., 1990, 9, 675-677

7. C. Hsieh and W. Wu: ‘Discussing the precipitation behavior of σ phase using diffusion equation and thermodynamic simulation in dissimilar stainless steels’, J. Alloys Compounds, 2010, 506, 820-825

8. C.C.Xu, G.Hu and W.-Y Ng: ‘Relationship between the martensite phase transition and pitting susceptibility of AISI-321 stainless steel in acidic solutions of NaCl’, Mater. Sci., 2004, 40, 252-259

9. J. K. L. Lai and M. Meshkat: ’Kinetics of precipitation of χ-phase and $M_{23}C_6$ carbide in a cast of Type 316 stainless steel’, Met. Sci.,1978, 12, 415-420

10. Y. Minami, H. Kimura and Y. Ihara: ’ Microstructural changes in austenitic stainless steels during long-term aging’, J. Mater. Sci. Technol, 1986, 2, 795-806

11. D. Dyson: ‘Use of CDM in materials modeling and component creep life prediction’, J. Press. Vess-T. ASME., 2000, 122, 28-296